Can even-membered liquid crystal dimers exhibit the twist-bend nematic phase? The preparation and properties of disulphide and thioether linked dimers

Naila Tufaha, Calum J. Gibb, John M. D. Storey & Corrie T. Imrie

Taylor & Francis
Taylor & Francis Group

🔓 OPEN ACCESS | Check for updates

Can even-membered liquid crystal dimers exhibit the twist-bend nematic phase? The preparation and properties of disulphide and thioether linked dimers

Naila Tufaha [iD], Calum J. Gibb, John M. D. Storey and Corrie T. Imrie [iD]

Department of Chemistry, School of Natural and Computing Sciences, University of Aberdeen, Aberdeen, UK

ABSTRACT

Cyanobiphenyl-based liquid crystal dimers containing a disulfide link in the spacer, the 4-[4-[2-[2-[4-(4-cyanophenyl)phenyl]alkyldisulfanyl]alkyl]-phenyl]benzonitriles (CBnSSnCB), are reported. The alkyl fragment is varied from two to nine carbon atoms, and all eight homologues exhibit nematic behaviour. In addition, the dimer containing heptamethylene fragments (CB7SS7CB) exhibits a twist-bend nematic phase despite having an even-membered spacer. The values of the nematic–isotropic transition temperature, T_{NI}, are higher for dimers containing an odd number of carbon atoms in each alkyl fragment. This surprising behaviour is interpreted in terms of the C-S-S-C torsion angle being around 88° that ensures that the molecular shape is bent irrespective of the parity of the alkyl fragments. For odd-membered fragments, however, the average shape is less bent and higher values of T_{NI} are observed. The more uniform molecular curvature of CB7SS7CB accounts for the observation of the N_{TB} phase. We also report the behaviour of two members of the 4-[4-[3-[2-[4-(4-cyanophenyl)phenyl]alkyldisulfanyl]-alkyl]phenyl]benzonitriles (CBnSmCB) which contain a thioether link embedded in the spacer. Both dimers exhibited nematic behaviour. The thioether link reduces the value of T_{NI} compared to that of the dimer with an alkyl spacer. A much larger decrease in the nematic-twist-bend nematic temperature is observed and is attributed to a change in shape.
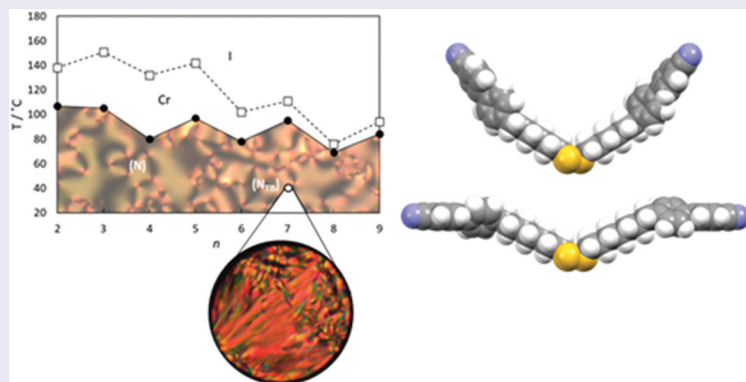
Introduction

Liquid crystal dimers consist of molecules containing two mesogenic units connected by a flexible spacer, most commonly an alkyl chain. These show very different behaviour to conventional low molar mass liquid crystals consisting of molecules containing a single mesogenic unit attached to which are one or two terminal alkyl chains [1,2]. The archetypal behaviour of a series of dimers on varying the number of methylene units in the spacer shows pronounced alternations in the values of, for example, the nematic–isotropic transition temperature, T_{NI}, and the associated scaled entropy change, $\Delta S_{NI}/R$. Dimers having an even number of methylene units in the spacer show the higher values. To a first approximation, the alternation in, for example, T_{NI} may be understood in terms of the average shape of the dimer and how this is governed by the parity of the spacer. Thus, for an even-membered spacer, the two mesogenic units are more

or less parallel, and the dimer is essentially linear. By contrast, in an odd-membered dimer, the two mesogenic units are inclined with respect to each other and the molecule is bent. The linear even-membered dimer is considered to be more compatible with the nematic environment, and hence higher values of T_{NI} are observed. Such a simple explanation neglects the inherent flexibility of the spacer but will suffice for our purposes [3].

Bent odd-membered dimers have attracted particular interest in recent years following the discovery of the fascinating twist-bend nematic, N_{TB}, phase for the dimer CB7CB that consists of two cyanobiphenyl moieties attached through a heptamethylene spacer [4–6]. This discovery confirmed the predictions of the N_{TB} phase made independently by Meyer [7] and Dozov [8]. In the N_{TB} phase, the directors spontaneously form a helix and are tilted with respect to the helical axis. Given that chiral formation is spontaneous, an equal number of left- and right-handed helices are expected. This double degeneracy may be removed, however, either by the addition of a chiral dopant or the introduction of chirality into the molecular structure, and the chiral twist-bend nematic phase is obtained [9–12]. A great many odd-membered dimers have now been shown to exhibit the N_{TB} phase (see for recent examples [13–23]), and it is widely accepted that their bent shape is the prerequisite for its observation. Indeed, molecular curvature is a common feature to the range of other structures known to support the N_{TB} phase including rigid bent core materials [24,25], hydrogen bonded systems [26–28], higher oligomers [29–34] and polymers [35]. Most recently, significant interest has focused on the incorporation of sulfur atoms into structures expected to exhibit the N_{TB} phase (see, for example, [36–47]).

It is often stated, therefore, that odd-membered dimers may exhibit the N_{TB} phase, whereas their even-membered counterparts cannot. This assumes that varying the parity of the spacer sees the average molecular shape change from being essentially linear to bent. It is known, however, that dimers containing a disulfide link in the spacer behave quite differently, although very few examples of such dimers and higher oligomers have been reported in the literature [48–54]. Specifically, the preferred conformation around the S-S link ensures that a dimer in which an even number of atoms connects the two mesogenic units is bent. It has not been established, however, to what extent the liquid crystalline environment can control the conformational distribution of this highly flexible link, and to investigate this, here we report the synthesis and characterisation of the 4-[4-[2-[2-[4-(4-cyanophenyl)phenyl]alkyldisulfanyl]alkyl]phenyl]benzonitriles, see Figure 1(a). We refer to these dimers using the acronym CB*n*SS*n*CB in which CB denotes a cyanobiphenyl fragment, *n* the number of carbon atoms in each alkyl chain, and SS the disulfide link. We have connected the spacer to the mesogenic units using methylene linkages as this is known to promote twist-bend nematic behaviour [55]. We stress that all the members in the CB*n*SS*n*CB series contain an even number of atoms linking their mesogenic units irrespective of the value of *n*. For comparison, we also report the transitional properties of two dimers containing a thioether link in the spacer, the 4-[4-[3-[2-[4-(4-cyanophenyl)phenyl]alkyldisulfanyl]alkyl]phenyl]benzonitriles, see Figure 1(b). These are referred to using the acronym CB*n*S*m*CB in which *n* - and *m* refer to the number of carbon atoms in each alkyl chain and S to the sulfur atom. In the two dimers reported, both *n* and *m* are odd such that the overall length of the spacer is odd. To our knowledge, just one dimer having
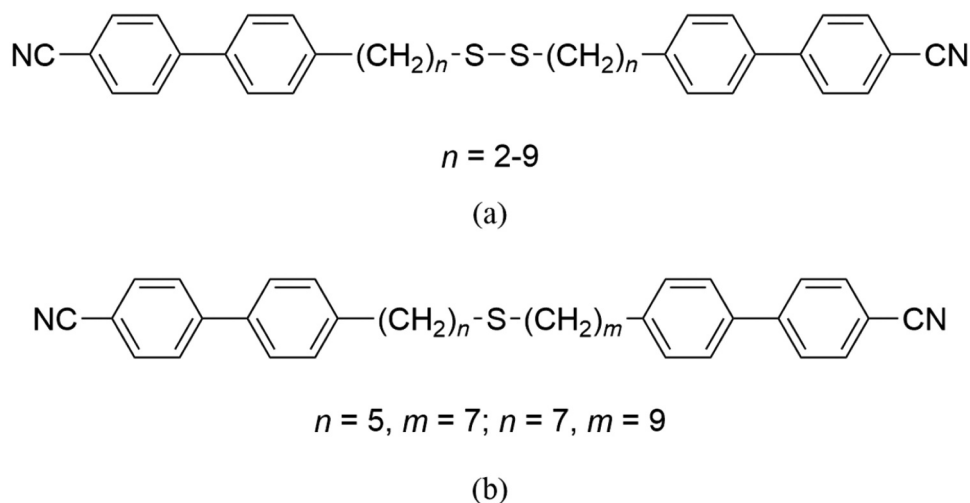

n = 2-9

(a)

n = 5, m = 7; n = 7, m = 9

(b)

Figure 1. The molecular structures of (a) the CB*n*SS*n*CB and (b) the CB*n*S*m*CB dimers.

a spacer containing an embedded thioether link has been reported, and this was not liquid crystalline [36].

Experimental

The synthetic route used to prepare the CB*n*SS*n*CB series is shown in Scheme 1. The preparation of the ω-bromo-1-(4-cyanobiphenyl-4'-yl) alkanes has been described in detail elsewhere [56]. The syntheses of the ω-(4-cyanobiphenyl-4'–yl)alkyl-1-thiols and their subsequent oxidative coupling to form the target dimers followed the procedures described by Lee et al. [51]. The synthetic route used to prepare the CB*n*S*m*CB dimers is shown in Scheme 2 and described elsewhere by Cruickshank et al. [45]. Complete descriptions of the synthetic procedures including the quantities of reagents used, yields of the final products and their intermediates, and structural characterisation data can be found in the Supplemental Information.

Structural and purity characterisation

The structures of the final products and their intermediates were confirmed using ^{1}H and ^{13}C NMR spectroscopy using a 400 MHz Bruker Advance III HD NMR spectrometer, and by Fourier-transform infrared spectroscopy using a Perkin Elmer Spectrum Two FTIR with an ATR diamond cell. A Biotage®Selekt system equipped with pre-packed silica columns, Biotage®Sfär High Capacity Duo 20 μm 100 g, 50 g or 10 g, with a flow rate of 120 ml/min was used to purify crude products. The purity of the final products was verified using either
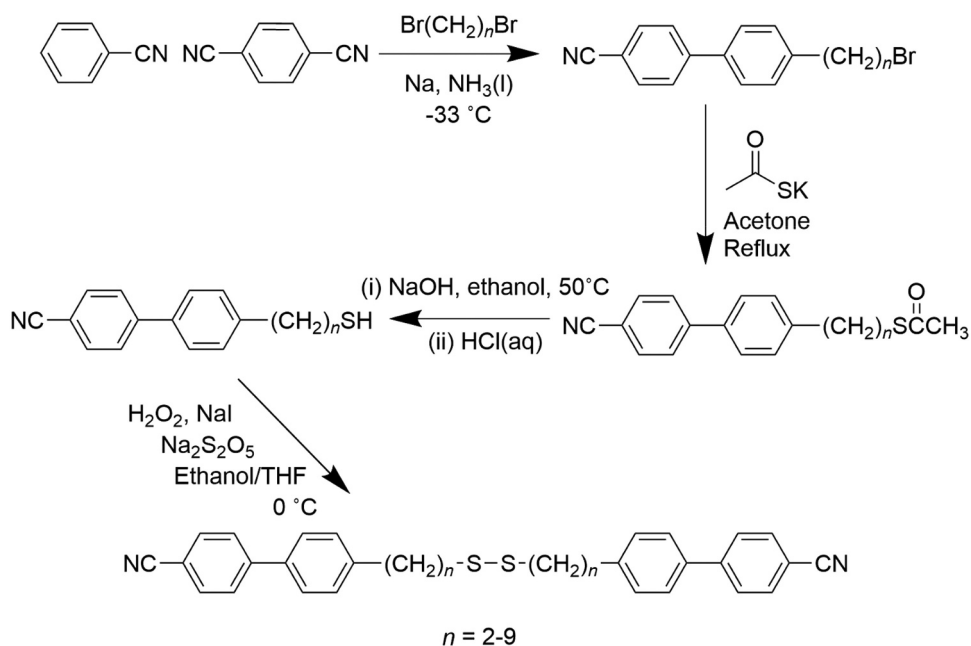
Scheme 1. The synthetic route used to prepare the CB*n*SS*n*CB series.
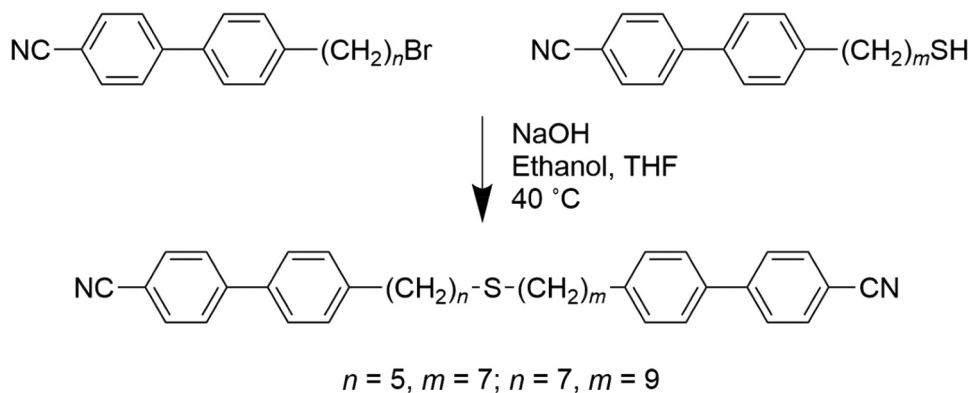
Scheme 2. The synthetic route used to prepare the CB*n*S*m*CB dimers.

high-resolution mass spectrometry using a Waters XEVO G2 QToF mass spectrometer operated by Dr Morag Douglas (University of Aberdeen) or by elemental analysis using an Elementar vario MICRO cube at the Sheffield Analytical and Scientific Services. Samples were analysed in duplicate for carbon, hydrogen, nitrogen and sulfur.

Thermal characterisation

Differential scanning calorimetry (DSC) was performed using a Mettler Toledo DSC1 differential scanning calorimeter, equipped with a TSO 801RO sample robot. The instrument was calibrated using indium and zinc standards. All the analyses performed used a heating profile composed of heat, cool and reheat segments with a 3-min isotherm between each segment, and a heating rate of $10°C$ min^{-1} under nitrogen gas. The thermal data reported were extracted from the cooling trace and the second heating trace. The data reported are average values measured for two different samples.

Polarised light microscopy was performed using an Olympus BH2 polarising optical microscope equipped with a Linkam TMS 92 hot stage. The samples were viewed either sandwiched between untreated glass microscope slides, or in cells of either 1.6 or 3 μm thickness, and coated with ITO conducting and polymer aligning layers.

Computational methods

Quantum mechanical density functional theory calculations were performed to determine the geometric parameters and electronic properties of the CBnSSnCB and CBnSmCB dimers. Geometry optimisation was performed using Gaussian G09W [57] at the B3LYP/6-311 G(d,p) level of theory. For the disulfide dimer CB4SS4CB, the all-trans conformation was tested by locking the CSSC torsion angle at the B3LYP/6-31 G(d) level of theory and compared with the non-constrained molecule at the same level of theory. For visualisation of the models, Mercury [58] and QuteMol [59] were used, while for visualisation of ball-and-stick models, electrostatic potential surfaces and dipole moments, GaussView 5 [60] was used.

Results and discussion

The CBnSSnCB series

The transitional properties of the CBnSSnCB series are listed in Table 1, and all eight homologues exhibit a monotropic nematic phase. This was assigned on the basis of the observation of a characteristic schlieren texture

Table 1. The temperatures and associated scaled entropy changes of the CBnSSnCB series. The data have been measured using DSC unless stated otherwise.

n	$T_{Crl}/°C$	$T_{N_{TB}N}/°C$	$T_{NI}/°C$	$\Delta S_{Crl}/R$	$\Delta S_{NI}/R$
2	138	–	107*	8.91	–
3	151	–	105	9.37	1.04
4	132	–	80*	12.5	–
5	142	–	97*	12.6	–
6	102	–	78	10.6	0.85
7	111	40*	95	16.8	–
8	76	–	69	17.4	1.39
9	94	–	84	17.7	2.04

*Measured using the polarised optical microscope.

containing both two and four brush point singularities and which flashed when subjected to mechanical stress when sandwiched between untreated glass slides; a representative texture of the nematic phase is shown in Figure 2.

Upon cooling isolated droplets of the nematic phase shown by CB7SS7CB, the schlieren texture changed to give a rather blocky texture at 40°C, see Figure 3. This was a reversible change upon heating, and is strongly suggestive of a nematic–twist-bend nematic, N_{TB}, phase transition [55]. Upon cooling, this lower temperature phase, crystallisation occurred rapidly at around 38°C. To confirm the assignment of the lower temperature liquid crystal phase, a binary phase diagram was constructed using mixtures of CB7SS7CB and CB15CB [61], the structure of which is shown in Figure 4. CB15CB has been characterised using a range of techniques including resonant soft X-ray scattering studies (RSoX) confirming its phase behaviour: it melts into the N_{TB} phase at 96°C, $T_{N_{TB}N} = 103°C$ and $T_{NI} = 121°C$. CB15CB was selected for this purpose given its similar spacer length. Complete miscibility of the two materials was observed over the whole composition range investigated, and each binary mixture exhibited two nematic phases. At higher temperatures, a conventional N phase was seen and identified based on the observation of the characteristic schlieren texture described earlier. At lower temperatures, the N_{TB} phase was observed, and identified by the formation of a brushstroke schlieren texture, see Figure 5. At the N-N_{TB} phase transition, there was a cessation of the optical flickering associated with director fluctuations in the N phase. The binary phase diagram constructed using these mixtures is shown in Figure 6. The melting points of the mixtures show eutectic-like behaviour. The nematic–isotropic transition temperatures decrease in essentially a linear manner upon decreasing the mole fraction of CB15CB, X_{CB15CB}, in the mixture. The values of the twist-bend nematic–nematic transition temperature, $T_{N_{TB}N}$, also decrease in essentially a linear fashion on decreasing X_{CB15CB} although we note that these data are somewhat more scattered. The extrapolated value of $T_{N_{TB}N}$ for CB7SS7CB based on this phase diagram is 40°C, in
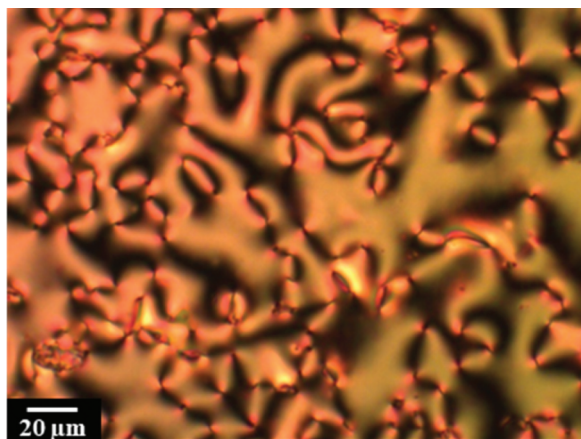
Figure 2. (Colour online) The schlieren texture of the nematic phase shown by CB6SS6CB ($T = 77°C$).

excellent agreement with the value measured experimentally, confirming the phase assignment.

The dependence of the transition temperatures on the number of methylene units, n, in each alkyl segment for the CBnSSnCB series is shown in Figure 7. Both the values of the melting point and T_{NI} tend to decrease on increasing n, and superimposed upon this is an alternation in which the odd members of n show the higher values. As we described earlier, the alternation in the value of T_{NI} on increasing the number of methylene units in the spacer for a series of dimers may be attributed to the change in the shape of the dimer as the parity of the spacer changes [1,2]. For the CBnSSnCB series, however, two methylene units are added each time, and the parity of the spacer remains constant with an even number of atoms always connecting the two cyanobiphenyl units. Within this framework, the odd-even effects seen for the melting points and values of T_{NI} on increasing n appear counter-intuitive. Similar behaviour has been observed for other dimers containing a disulfide linkage in the spacer [51,54]. Furthermore, we have seen that CB7SS7CB shows the N_{TB} phase, and given that this is an even-member dimer, this is a highly surprising observation.
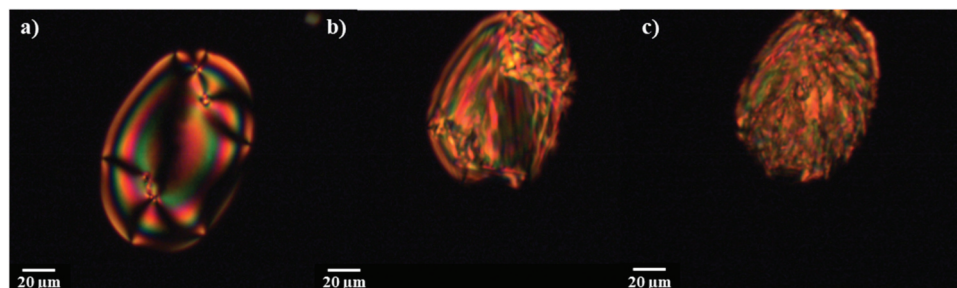

Figure 3. (Colour online) The optical textures seen for isolated droplets of CB7SS7CB in the (a) nematic ($T = 94°C$), (b) twist-bend nematic ($T = 40°C$) and (c) crystal phases ($T = 38°C$).
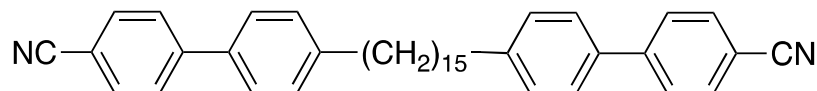

Figure 4. Molecular structure of CB15CB.

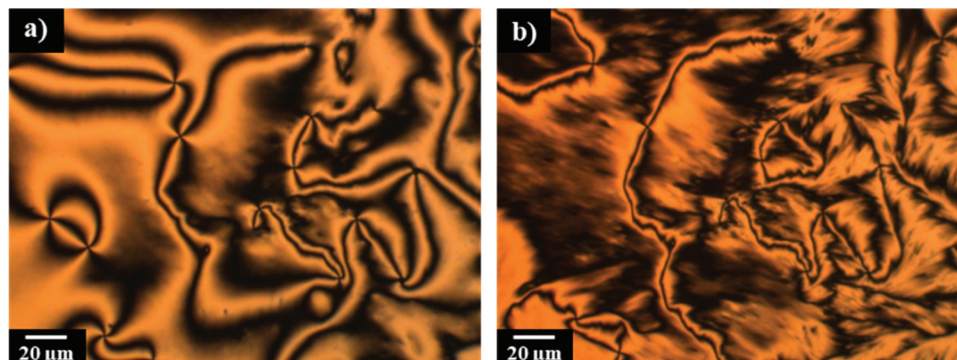**Figure 5.** (Colour online) (a) The schlieren texture of the N phase ($T = 87°C$) and (b) the brushstroke texture of the N_{TB} phase ($T = 106°C$) for the $X_{CB15CB} = 0.6$ mixture.
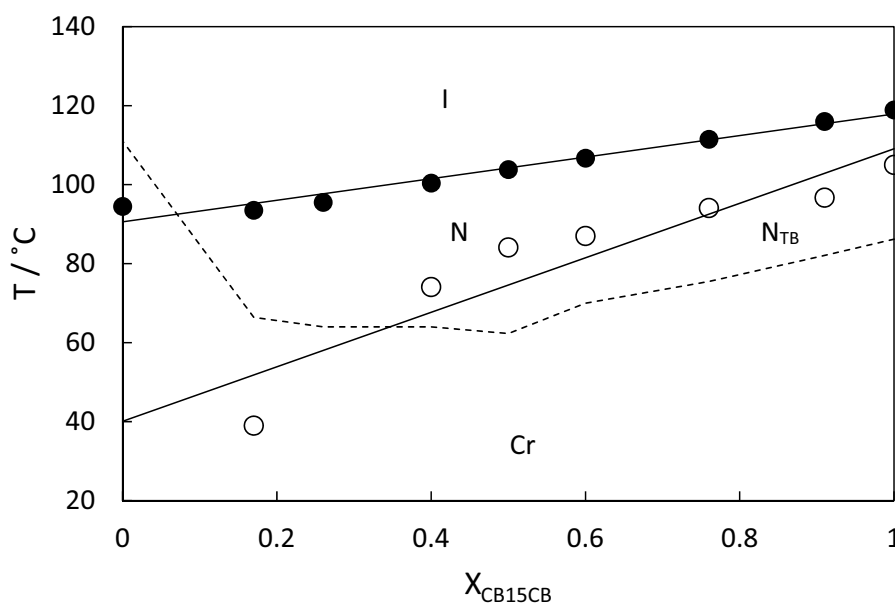
Figure 6. Binary phase diagram for mixtures of CB7SS7CB and CB15CB plotted as a function of the mole fraction CB15CB, X_{CB15CB}, in the mixture. The filled circles indicate nematic–isotropic transitions, open circles twist-bend nematic–nematic transitions and the broken line connects the melting points.
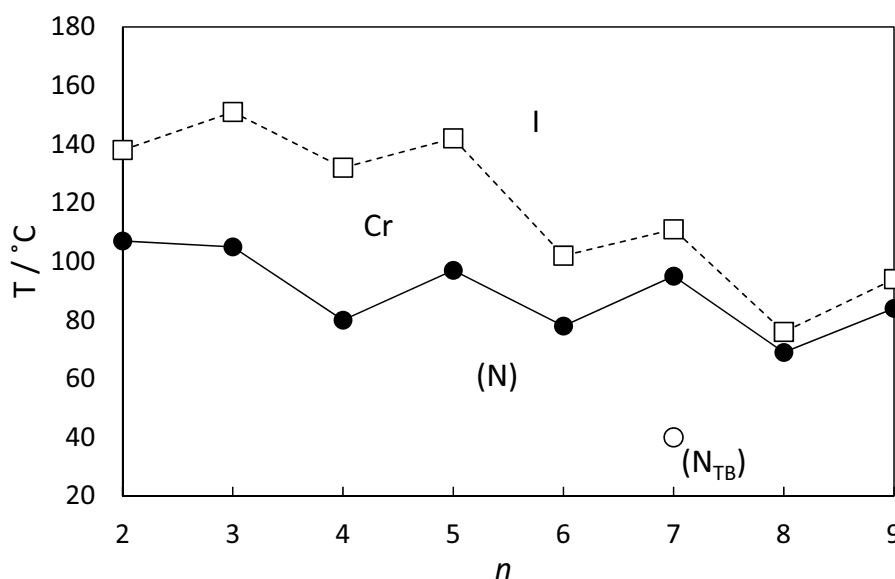

Figure 7. The dependence of the transition temperatures on the number of carbon atoms in each alkyl segment, n, for the CBnSSnCB series. The melting points are connected by the broken line and the values of T_{NI} by the solid line. The open circle denotes the $N_{TB}N$ transition seen for CB7SS7CB.

In order to understand the surprising behaviour seen in Figure 7, we calculated the molecular structures of CB6SS6CB and CB7SS7CB, and these are shown in Figure 8. The C-S-S-C torsion angle in both dimers is around 88° and presumably arises from lone pair repulsions of the sulfur atoms. This angle does not depend on either the chain length, n, or parity as neither increases the steric bulk around the disulfide bond. Although the disulfide torsion angle does not vary with n, it is clear in

Figure 8 that two significantly different shapes are adopted by these dimers depending on the parity of n. CB6SS6CB adopts a U-shape in which there is a twist along the molecular axis, Figure 8(a), whereas CB7SS7CB is more linear and the two mesogenic units are more or less parallel. This difference arises because the bent nature of the odd-membered methylene fragments in CB7SS7CB counters the effect of the dihedral angle associated with the disulfide bond, whereas the
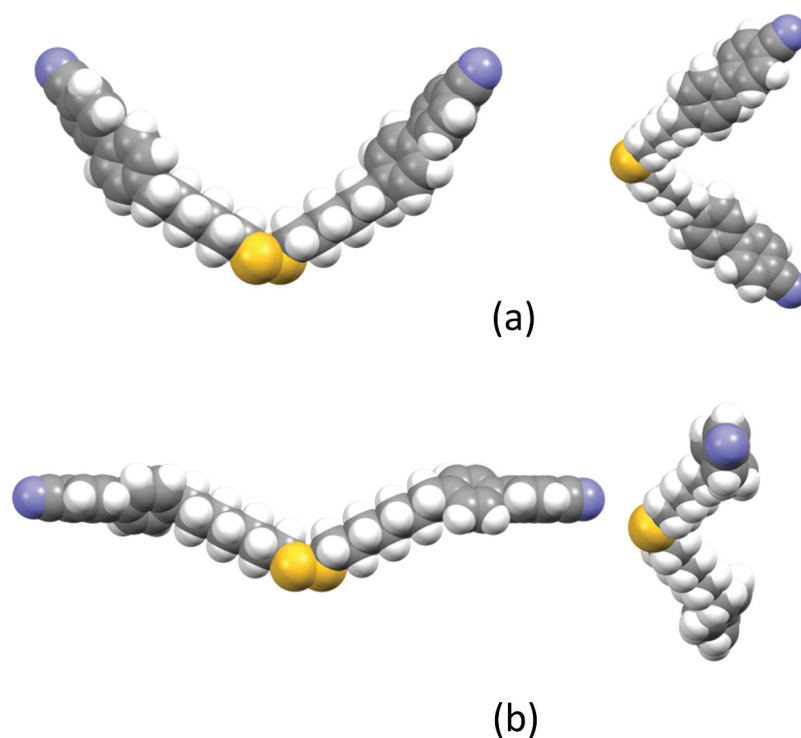
Figure 8. (Colour online) Molecular structures of (a) CB6SS6CB and (b) CB7SS7CB as determined by geometry optimization (DFT/B3LYP/6-311G(d,p)). The views on the right are along the S-S bond.

linear alkyl fragments in CB6SS6CB simply extend the molecule and the dispositions of the mesogenic units reflect the dihedral angle arising from the disulfide bond. We note that constraining the disulfide bond to an all-*trans* conformation increased the calculated energy, supporting the view that it has a preference for the *gauche* conformation in systems lacking steric congestion [62].

Thus, the alternation in the values of T_{NI} on varying the parity of n seen in Figure 7 may be interpreted in terms of the accompanying change in molecular shape between two bent shapes, see Figure 8. For odd members of n, the overall molecular shape is less bent and, hence, higher values of T_{NI} are seen. This interpretation is supported by the values of the scaled entropy change associated with the nematic–isotropic transition, $\Delta S_{NI}/R$, listed in Table 1. For the CBnCB series, a pronounced alternation is observed in $\Delta S_{NI}/R$ on varying the parity of n; for example, for CB6CB, $\Delta S_{NI}/R$ is 2.63, whereas for CB7CB, it is just 0.22 [63]. The much larger value of $\Delta S_{NI}/R$ for CB6CB, an even-membered linear dimer, reflects a higher conformational contribution to the overall entropy change, and more significantly, a larger long-range orientational order [64,65]. For the CBnSSnCB dimers, the values of $\Delta S_{NI}/R$ are more in keeping with those observed for odd-

membered dimers; for example, for dimers of comparable length, the value of $\Delta S_{NI}/R$ is 0.91 for CB13CB [63] and very similar to that of CB6SS6CB of 0.85. This reinforces the view that the CBnSSnCB dimers exist in bent conformations. Furthermore, the larger values of $\Delta S_{NI}/R$ shown by the dimers with an odd value n than those of similar length but even values of n reflect the difference in molecular biaxiality [66,67] supporting the view that for odd values of n, the dimers are, on average, less bent.

A twist-bend nematic phase has been observed for just CB7SS7CB. We have noted already that molecular curvature is a prerequisite for the observation of the N_{TB} phase and it may appear counter-intuitive that the N_{TB} phase is observed for the less bent of these dimers. It has been established, however, that the uniformity of molecular curvature is an important consideration on the stability of the N_{TB} phase [68], and this is greater for dimers having an odd value of n, see Figure 8. We also note that the less bent shape of CB7SS7CB compared to, for example, CB6SS6CB, Figure 8, facilitates better interactions between the mesogenic units, and this compensates for the loss of entropy due to the additional polar order in the N_{TB} phase. This, in turn, counteracts the larger bend angle in CB7SS7CB than CB6SS6CB such that a higher value of T_{NTBN} is observed for the more linear of these molecules.

We note that a nematic–nematic transition was reported for the ether-linked analogue of CB7SS7CB, namely CBO6SS6OCB [52,53], on the basis of the temperature dependence of the birefringence. Specifically, a small discontinuous decrease in the nematic range was seen, indicative of a weak first-order transition, after which the value of birefringence continued to increase [53]. Although it may be tempting to speculate that this is also an N_{TB}-N transition, this profile is not consistent with that characteristically observed for the N-N_{TB} transition, which is often associated with a small jump to higher values in the birefringence, and a subsequent decrease on cooling the N_{TB} phase. This characteristic behaviour has been accounted for in terms of the formation of the oblique helix [69]. It would appear, therefore, that the N-N transition seen for CBO6SS6OCB is not a N_{TB}-N transition.

The CBnSmCB dimers

We now turn our attention to dimers containing a thioether link in their spacer, CB5S7CB and CB7S9CB (Figure 1) and their transitional properties are listed in Table 2. Both dimers showed a conventional nematic phase, identified on the basis of the observation of a characteristic schlieren texture described earlier, and shown in Figure 9. Upon cooling the nematic phase of both dimers, no other liquid crystal phase was seen prior to crystallisation. To estimate a virtual value of $T_{N_{TB}N}$ for CB5S7CB, a phase diagram was constructed for binary mixtures of CB5S7CB and CB13CB [63], see Figure 10. The latter was chosen given the similarity in spacer length. The mixtures exhibited a monotropic conventional nematic phase across the complete composition range, and a monotropic twist-bend nematic phase for mixtures with mole fraction CB13CB, $X_{CB13CB} \geq 0.40$. The phases were assigned based on the observation of characteristic optical textures as described earlier. The melting points of the mixtures show only a weak dependence on composition. The values of T_{NI} and $T_{N_{TB}N}$ decrease in essentially a linear fashion on decreasing X_{CB13CB}, and the gradient of the $T_{N_{TB}N}$ line is larger. The virtual value of $T_{N_{TB}N}$ for CB5S7CB estimated by extrapolation of the
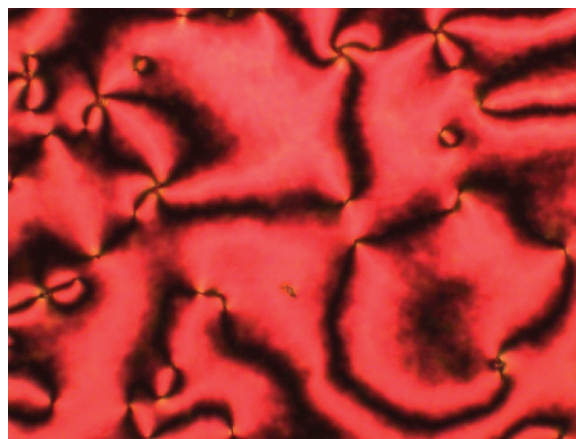

Figure 9. (Colour online) The nematic schlieren texture exhibited by CB7S9CB ($T = 95°C$).

$T_{N_{TB}N}$ line is 73°C although we note that this extrapolation is rather long and so the value should be treated with some degree of caution. Attempts to confirm this estimated $T_{N_{TB}N}$ were unsuccessful because the nematic phase of CB5S7CB could not be supercooled to this temperature prior to crystallisation.

The melting point of CB5S7CB is 13°C higher than that of CB13CB, whereas this is reversed on comparing the melting points of CB7S9CB and CB17CB, the latter being 7°C lower. The insertion of the thioether link into the spacer reduces the value of T_{NI} compared to that of the corresponding dimer with an alkyl spacer by around 13°C. A much larger effect is seen, however, in the value of $T_{N_{TB}N}$. For CB5S7CB, the estimated value of $T_{N_{TB}N}$ is some 38°C lower than that of CB13CB. A similar reduction in $T_{N_{TB}N}$ is observed for CB7S9CB on comparing the lowest temperature to which the N phase may be cooled prior to crystallisation to the value of $T_{N_{TB}N}$ observed for CB17CB.

The space filling model for CB7S9CB with the spacer in the all-*trans* conformation as determined by geometry optimisation is shown in Figure 11. It has been suggested that a *gauche* conformation about the CH_2-S bond is slightly favoured by around 0.4 kJ mol^{-1}, and that this arises from a favourable electrostatic interaction between the negatively charged sulfur atoms and positively charged CH_2 groups [70]. As described in more detail elsewhere [21], however, this value is likely to be substantially different in a liquid crystal environment which will preferentially select more linear conformations [71]. Thus, we consider the all-*trans* conformation to be a better representation of the average molecular shape in discussing the transitional properties of these dimers. The CSC bond angle is around 100° compared to the CCC bond angle of 109.5° and this induces a slight curvature of the spacer compared to an

Table 2. The transition temperatures and associated scaled entropy changes of the CBnSmCB series. The data have been measured using DSC. The transitional properties of the members of the CBnCB series having the same spacer length are also listed.

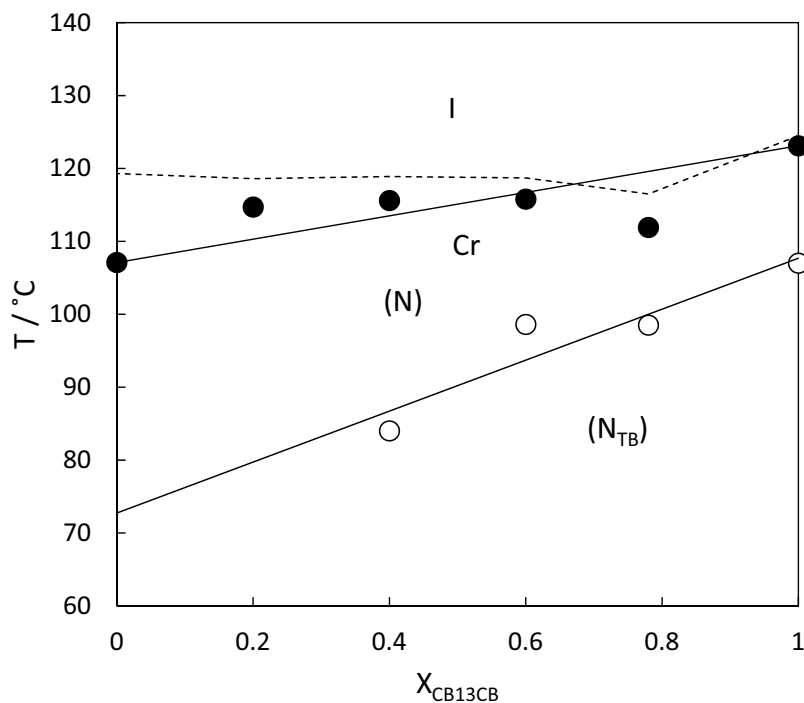| Dimer	$T_{Cr\text{-}}$ /°C	$\Delta S_{CrI}/R$	$T_{N_{TB}N}$/°C	T_{NI}/°C	$\Delta S_{NI}/R$	Ref
CB5S7CB	119	11.0	–	(107)	1.14	
CB13CB	106	9.40	(105)	122	0.91	[63]
CB7S9CB	92	13.6	–	105	1.55	
CB17CB	99	15.3	(97)	117	1.45	[61]

Figure 10. Binary phase diagram for mixtures of CB5S7CB and CB13CB plotted as a function of the mole fraction CB13CB, X_{CB13CB}, in the mixture. The filled circles indicate nematic–isotropic transitions, open circles twist-bend nematic–nematic transitions and the broken line connects the melting points.
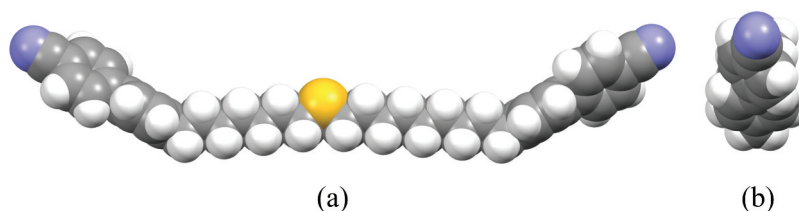

Figure 11. (Colour online) (a) Space filling model for CB7S9CB and (b) viewed along the spacer.

all-*trans* alkyl spacer. This distortion opposes the overall molecular curvature. As we noted earlier, the uniformity of molecular curvature appears to be an important factor in stabilising the N_{TB} phase and this small change in shape between the CB*n*CB and CB*n*S*m*CB dimers may account for the significantly lower values of $T_{N_{TB}N}$ seen for the latter, reinforcing the view that the N_{TB}-N transition is predominantly shape driven.

A second factor to be considered is the change in the electronic properties of the dimer associated with the insertion of the sulfur atom into the spacer. The calculated electrostatic potential surface for CB5S7CB is shown in Figure 12 alongside its ball-and-stick model showing the direction of the molecular dipole moment. The molecular dipole moments of CB5S7CB and CB7S9CB are 7.06 and 7.47 D, respectively, and these are higher than that calculated for CB17CB of 6.44 D but

oriented in the same direction [61]. It may have been anticipated that stronger dipole interactions between the CB*n*S*m*CB dimers would drive higher melting points, and this is indeed the case comparing CB5S7CB and CB13CB. Upon increasing the length of the alkyl fragments, however, this effect will be diluted, and the melting points are expected to become more similar as indeed they do. It should also be noted that the packing efficiency of the dimers will play a role in determining the melting points. The reduction in local packing efficiency arising from the insertion of the sulfur atom into the spacer is likely to be small given that the van der Waals volume of sulfur is around 10.8 $cm^3 mol^{-1}$ and similar to that of the CH_2 group of 10.23 $cm^3 mol^{-1}$ [72], and this difference may be accommodated, at least to some extent, by the increased flexibility of the thioether chain. This rather subtle combination of
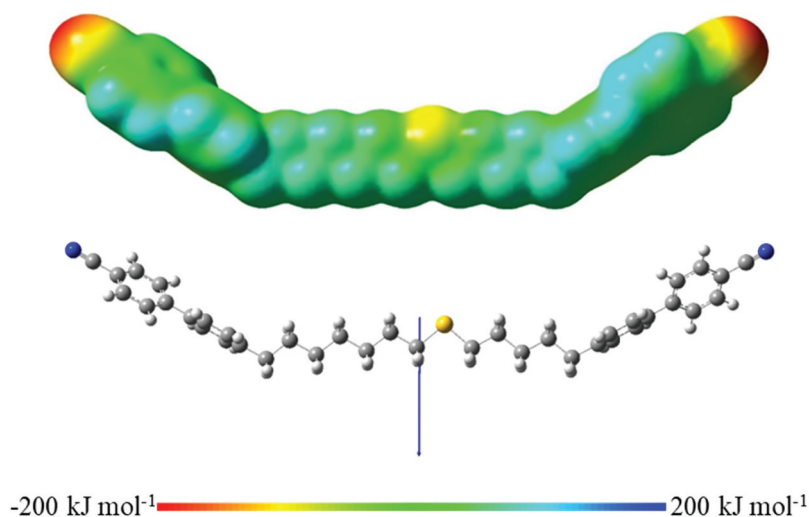
Figure 12. (Colour online) The electrostatic potential surface (top), and ball and stick model showing the molecular dipole moment (bottom) for the ground state all-*trans* conformation of CB5S7CB.

electronic and steric effects accounts for the less regular effects on the melting temperature seen for these dimers.

We now turn our attention to the nematic–isotropic transition, and as we have seen, the insertion of a sulfur atom into the spacer reduces this by around 13°C (Table 2). It is interesting to note that the insertion of a sulfur atom into the spacer of a semi-flexible main chain liquid crystal polymer reduces the value of the liquid crystal-isotropic transition temperature by around the same margin as seen for these dimers [73]. This reduction presumably reflects the reduction in shape anisotropy arising from the larger CSC bond angle and the larger sulfur atom as described earlier. It is possible that these effects will be offset, to some extent, by increased dipolar interactions. It is interesting to note that the values of $\Delta S_{NI}/R$ for the corresponding dimers with and without a sulfur atom are essentially the same, and wholly characteristic for an odd-membered dimer containing a long spacer. This strongly suggests that their respective shapes are rather similar.

Conclusions

In the introduction, we noted the widely held view that even-membered dimers cannot exhibit the N_{TB} phase. We have shown, however, that this statement must be used with care, and CB7SS7CB does indeed exhibit the N_{TB} phase even though the mesogenic units are linked by an even number of atoms. This surprising observation may be accounted for in terms of the torsion angle around the C-S-S-C bond, and how the bend this introduces into the molecular structure is counteracted by that associated with the odd-membered alkyl fragments. Although dimers containing both odd- and even-membered alkyl fragments are bent, those with odd-membered fragments are less bent and the curvature more uniform. This accounts for both the alternation in the values of T_{NI} on varying n in which odd values of n show the higher values, and the observation of the N_{TB} phase for CB7SS7CB. The shape change associated with insertion of a single sulfur atom into the alkyl spacer for the CB*n*S*m*CB dimers is much less pronounced, and consequently a smaller change in transitional properties is seen. These have been attributed to the combination of a reduction in shape anisotropy arising from the larger sulfur atom, and smaller CSC bond angle, coupled with increased dipolar interactions. As would be expected, the reduction in the stability of the N_{TB} phase is more pronounced given its particular sensitivity to molecular shape. It is also apparent that the behaviour of the dimers is rather similar to that of semi-flexible polymers, casting new light on the behaviour of the latter. The generality of our observations now has to be tested by the characterisation of a wider range of dimers including disulfide and thioether links in the spacer.

ORCID

Naila Tufaha http://orcid.org/0000-0003-4042-7458
Corrie T. Imrie http://orcid.org/0000-0001-6497-5243

References

[1] Imrie CT, Henderson PA. Liquid crystal dimers and higher oligomers: between monomers and polymers. Chem Soc Rev. 2007;36(12):2096–2124. doi: 10.1039/b714102e

[2] Imrie CT, Henderson PA, Yeap GY. Liquid crystal oligomers: going beyond dimers. Liq Cryst. 2009;36 (6–7):755–777. doi: 10.1080/02678290903157455

[3] Luckhurst GR. Liquid-crystal dimers and oligomers - experiment and theory. Macromol Symp. 1995;96:1–26. doi: 10.1002/masy.19950960103

[4] Cestari M, Diez-Berart S, Dunmur DA, et al. Phase behavior and properties of the liquid-crystal dimer 1",7"-bis(4-cyanobiphenyl-4'- yl) heptane: A twist-bend nematic liquid crystal. Phys Rev E. 2011;84:031704. doi: 10.1103/PhysRevE.84.031704

[5] Borshch V, Kim YK, Xiang J, et al. Nematic twist-bend phase with nanoscale modulation of molecular orientation. Nature Commun. 2013;4(1):2635. doi: 10.1038/ncomms3635

[6] Zhu CH, Tuchband MR, Young A, et al. Resonant Carbon K-Edge soft X-Ray scattering from lattice-free heliconical molecular ordering: soft dilative elasticity of the twist-bend liquid crystal phase. Phys Rev Lett. 2016;116 (14):147803. doi: 10.1103/PhysRevLett.116.147803

[7] Meyer RB. Structural problems in liquid crystal physics, les houches summer school in theoretical physics. In: Balian R, W G, editors. Molecular fluids. New York: Gordon and Breach; 1976. p. 273–373.

[8] Dozov I. On the spontaneous symmetry breaking in the mesophases of achiral banana-shaped molecules. Europhys Lett. 2001;56(2):247–253. doi: 10.1209/epl/i2001-00513-x

[9] Archbold CT, Davis EJ, Mandle RJ, et al. Chiral dopants and the twist-bend nematic phase - induction of novel mesomorphic behaviour in an apolar bimesogen. Soft Matter. 2015;11:7547–7557. doi: 10.1039/C5SM01935D

[10] Kasian NA, Lisetski LN, Gvozdovskyy IA. Twist-bend nematics and heliconical cholesterics: a physico-chemical analysis of phase transitions and related specific properties. Liq Cryst. 2022;49 (1):142–152. doi: 10.1080/02678292.2021.1970838

[11] Walker R, Pociecha D, Salamonczyk M, et al. Intrinsically chiral twist-bend nematogens: interplay of molecular and structural chirality in the N_{TB} phase. Chemphyschem. 2023;24:e202300105. doi: 10.1002/cphc.202300105

[12] Walker R, Pociecha D, Storey JMD, et al. The chiral twist-bend nematic phase (N*(TB)). Chem Eur J. 2019;25:13329–13335. doi: 10.1002/chem.201903014

[13] Alshammari AF, Pociecha D, Walker R, et al. New patterns of twist-bend liquid crystal phase behaviour: the synthesis and characterisation of the 1-(4-cyanobiphenyl-4'-yl)-10-(4-alkylaniline-benzylidene-4'-oxy) decanes (CB10O.m). Soft Matter. 2022;18:4679–4688. doi: 10.1039/D2SM00162D

[14] Forsyth E, Paterson DA, Cruickshank E, et al. Liquid crystal dimers and the twist-bend nematic phase: on the role of spacers and terminal alkyl chains. J Molec Liq. 2020;320:114391. doi: 10.1016/j.molliq.2020.114391

[15] Pociecha D, Vaupotic N, Majewska M, et al. Photonic bandgap in achiral liquid crystals-a twist on a twist. Adv Mater. 2021;33:2103288. doi: 10.1002/adma.202103288

[16] Walker R, Majewska M, Pociecha D, et al. Twist-Bend nematic glasses: the synthesis and characterisation of pyrene-based nonsymmetric dimers. Chemphyschem. 2021;22(5):461–470. doi: 10.1002/cphc.202000993

[17] Walker R, Pociecha D, Strachan GJ, et al. Molecular curvature, specific intermolecular interactions and the twist-bend nematic phase: the synthesis and characterisation of the 1-(4-cyanobiphenyl-4-yl)-6-(4-alkylanilinebenzylidene-4-oxy)hexanes (CB6O.m). Soft Matter. 2019;15:3188–3197. doi: 10.1039/C9SM00026G

[18] Mandle RJ. Designing liquid-crystalline oligomers to exhibit twist-bend modulated nematic phases. Chem Rec. 2018;18(9):1341–1349. doi: 10.1002/tcr.201800010

[19] Mandle RJ. A Ten-Year perspective on twist-bend nematic materials. Molecules. 2022;27(9):2689. doi: 10.3390/molecules27092689

[20] Pocock EE, Mandle RJ, Goodby JW. Molecular shape as a means to control the incidence of the nanostructured twist bend phase. Soft Matter. 2018;14(13):2508–2514. doi: 10.1039/C7SM02364B

[21] Paterson DA, Walker R, Abberley JP, et al. Azobenzene-based liquid crystal dimers and the twist-bend nematic phase. Liq Cryst. 2017;44:2060–2078. doi: 10.1080/02678292.2017.1366075

[22] Knezevic A, Dokli I, Novak J, et al. Fluorinated twist-bend nematogens: the role of intermolecular interaction. Liq Cryst. 2021;48(5):756–766. doi: 10.1080/02678292.2020.1817585

[23] Babakhanova G, Wang H, Rajabi M, et al. Elastic and electro-optical properties of flexible fluorinated dimers with negative dielectric anisotropy. Liq Cryst. 2022;49 (7–9):982–994. doi: 10.1080/02678292.2021.1973602

[24] Chen D, Nakata M, Shao R, et al. Twist-bend heliconical chiral nematic liquid crystal phase of an achiral rigid bent-core mesogen. Phys Rev E. 2014;89(2):022506. doi: 10.1103/PhysRevE.89.022506

[25] Sreenilayam SP, Panov VP, Vij JK, et al. The N-TB phase in an achiral asymmetrical bent-core liquid crystal terminated with symmetric alkyl chains. Liq Cryst. 2017;44:244–253. doi: 10.1080/02678292.2016.1253878

[26] Walker R, Pociecha D, Abberley JP, et al. Spontaneous chirality through mixing achiral components: a twist-bend nematic phase driven by hydrogen-bonding between unlike components. Chem Commun. 2018;54 (27):3383–3386. doi: 10.1039/C8CC00525G

[27] Jansze SM, Martinez-Felipe A, Storey JMD, et al. A twist-bend nematic phase driven by hydrogen bonding. Angew Chem Int Ed. 2015;54:643–646. doi: 10.1002/anie.201409738

[28] Walker R, Pociecha D, Crawford CA, et al. Hydrogen bonding and the design of twist-bend nematogens. J Molec Liq. 2020;303:112630. doi: 10.1016/j.molliq.2020.112630

[29] Mandle RJ. The dependency of twist-bend nematic liquid crystals on molecular structure: a progression from dimers to trimers, oligomers and polymers. Soft Matter. 2016;12(38):7883–7901. doi: 10.1039/C6SM01772J

[30] Mandle RJ, Goodby JW. Progression from nano to macro science in soft matter systems: dimers to trimers and oligomers in twist-bend liquid crystals. RSC Adv. 2016;6(41):34885–34893. doi: 10.1039/C6RA03594A

[31] Mandle RJ, Goodby JW. A nanohelicoidal nematic liquid crystal formed by a non-linear duplexed hexamer. Angew Chem Int Ed. 2018;57 (24):7096–7100. doi: 10.1002/anie.201802881

[32] Simpson FP, Mandle RJ, Moore JN, et al. Investigating the cusp between the nano-and macro-sciences in supermolecular liquid-crystalline twist-bend nematogens. J Mater Chem C. 2017;5:5102–5110. doi: 10.1039/C7TC00516D

[33] Tuchband MR, Paterson DA, Salamonczykc M, et al. Distinct differences in the nanoscale behaviors of the twist-bend liquid crystal phase of a flexible linear trimer and homologous dimer. Proc Nat Acad Sci USA. 2019;116:10698–10704. doi: 10.1073/pnas.1821372116

[34] Majewska MM, Forsyth E, Pociecha D, et al. Controlling spontaneous chirality in achiral materials: liquid crystal oligomers and the heliconical twist-bend nematic phase. Chem Commun. 2022;58(34):5285–5288. doi: 10.1039/D1CC07012F

[35] Stevenson WD, An JG, Zeng XB, et al. Twist-bend nematic phase in biphenylethane-based copolyethers. Soft Matter. 2018;14(16):3003–3011. doi: 10.1039/C7SM02525D

[36] Arakawa Y, Komatsu K, Inui S, et al. Thioether-linked liquid crystal dimers and trimers: the twist-bend nematic phase. J Mol Struct. 2020;1199:1199. doi: 10.1016/j.molstruc.2019.126913

[37] Arakawa Y, Komatsu K, Shiba T, et al. Methylene- and thioether-linked cyanobiphenyl-based liquid crystal dimers CBnSCB exhibiting room temperature twist-bend nematic phases and glasses. Mater Adv. 2021;2(5):1760–1773. doi: 10.1039/D0MA00990C

[38] Arakawa Y, Ishida Y, Komatsu K, et al. Thioether-linked benzylideneaniline-based twist-bend nematic liquid crystal dimers: insights into spacer lengths, mesogenic arm structures, and linkage types. Tetrahedron. 2021;95:132351. doi: 10.1016/j.tet.2021.132351

[39] Arakawa Y, Ishida Y, Tsuji H. Ether- and thioether-linked naphthalene-based liquid-crystal dimers: influence of chalcogen linkage and mesogenic-arm symmetry on the incidence and stability of the twist-bend nematic phase. Chem Eur J. 2020;26:3767–3775. doi: 10.1002/chem.201905208

[40] Arakawa Y, Komatsu K, Feng J, et al. Distinct twist-bend nematic phase behaviors associated with the ester-linkage direction of thioether-linked liquid crystal dimers. Mater Adv. 2021;2(1):261–272. doi: 10.1039/D0MA00746C

[41] Arakawa Y, Komatsu K, Ishida Y, et al. Carbonyl- and thioether-linked cyanobiphenyl-based liquid crystal dimers exhibiting twist-bend nematic phases. Tetrahedron. 2021;81:131870. doi: 10.1016/j.tet.2020.131870

[42] Arakawa Y, Komatsu K, Ishida Y, et al. Thioether-linked liquid crystal trimers: odd-even effects of spacers and the influence of thioether bonds on phase behavior. Materials. 2022;15:1709. doi: 10.3390/ma15051709

[43] Arakawa Y, Komatsu K, Ishida Y, et al. Thioether-linked azobenzene-based liquid crystal dimers exhibiting the twist-bend nematic phase over a wide temperature range. Liq Cryst. 2021;48(5):641–652. doi: 10.1080/02678292.2020.1800848

[44] Arakawa Y, Komatsu K, Shiba T, et al. Phase behaviors of classic liquid crystal dimers and trimers: alternate induction of smectic and twist-bend nematic phases depending on spacer parity for liquid crystal trimers. J Molec Liq. 2021;326:115319. doi: 10.1016/j.molliq.2021.115319

[45] Cruickshank E, Salamonczyk M, Pociecha D, et al. Sulfur-linked cyanobiphenyl-based liquid crystal dimers and the twist-bend nematic phase. Liq Cryst. 2019;46 (10):1595–1609. doi: 10.1080/02678292.2019.1641638

[46] Cruickshank E, Anderson K, Storey JMD, et al. Helical phases assembled from achiral molecules: twist-bend nematic and helical filamentary B-4 phases formed by mesogenic dimers. J Molec Liq. 2022;346:118180. doi: 10.1016/j.molliq.2021.118180

[47] Cruickshank E, Strachan GJ, Majewska MM, et al. The effects of alkylthio chains on the properties of symmetric liquid crystal dimers. New J Chem. 2023;47 (15):7356–7368. doi: 10.1039/D2NJ06252F

[48] Yeap GY, Osman F, Mahmood WAK, et al. Molecular structure-thermal behaviour relationship of dimers consisting of different terminal substituents and sulphur-sulphur linking group. J Mol Struct. 2014;1074:666–672. doi: 10.1016/j.molstruc.2014.03.071

[49] Osman F, Yeap GY, Takeuchi D. Synthesis and meso-morphic behaviour of new disulphide bridge 4-n-alkoxy-benzylidine-4'-bromoaniline. Liq Cryst. 2014;41:106–112. doi: 10.1080/02678292.2013.839833

[50] Yap PW, Osman F, Yeap GY, et al. Non-linear disulphide-centred S-shaped oligomers with inner and outer spacers connected by aromatic azo moieties. Liq Cryst. 2023;50:379–392. doi: 10.1080/02678292.2022.2127161

[51] Lee HC, Lu ZB, Henderson PA, et al. Cholesteryl-based liquid crystal dimers containing a sulfur-sulfur link in the flexible spacer. Liq Cryst. 2012;39:259–268. doi: 10.1080/02678292.2011.641753

[52] Kundu B, Pal SK, Kumar S, et al. Splay and bend elastic constants in the nematic phase of some disulfide bridged dimeric compounds. Phys Rev E. 2010;82 (6):061703. doi: 10.1103/PhysRevE.82.061703

[53] Kundu B, Pal SK, Kumar S, et al. Unusual odd-even effects depending on the monomer chain length in nematic liquid crystals made of rod-like dimers. Eur Phys Lett. 2009;85 (3):36002. doi: 10.1209/0295-5075/85/36002

[54] Pal SK, Raghunathan VA, Kumar S. Phase transitions in novel disulphide-bridged alkoxycyanobiphenyl dimers. Liq Cryst. 2007;34(2):135–141. doi: 10.1080/02678290601061280

[55] Henderson PA, Imrie CT. Methylene-linked liquid crystal dimers and the twist-bend nematic phase. Liq Cryst. 2011;38(11–12):1407–1414. doi: 10.1080/02678292.2011.624368

[56] Gibb CJ, Storey JM, Imrie CT. A convenient one-pot synthesis, and characterisation of the omega-bromo -1-(4-cyanobiphenyl-4'-yl) alkanes (CBnBr). Liq Cryst. 2022;49:1706–1716. doi: 10.1080/02678292.2022.2084568

[57] Frisch MJ, Trucks GW, Schlegel HB, et al. Gaussian 09 (Revision D.01). Wallingford (CT): Gaussian Inc; 2016.

[58] Macrae CF, Sovago I, Cottrell SJ, et al. Mercury 4.0: from visualization to analysis, design and prediction. J Appl Cryst. 2020;53(1):226–235. doi: 10.1107/S1600576719014092

[59] Tarini M, Cignoni P, Montani C. Ambient occlusion and edge cueing to enhance real time molecular visualization. IEEE Trans Vis Comp Graphics. 2006;12:1237–1244. doi: 10.1109/TVCG.2006.115

[60] Dennington R, Keith T, Millam J. Gauss view, Version 5. Shawnee Mission (KS): Semichem Inc; 2009.

[61] Cruickshank E. [PhD thesis]. University of Aberdeen; 2021.

[62] Jorgensen FS, Snyder JP. Disulfide conformational-analysis - nature of the S-S rotation barrier. Tetrahedron. 1979;35:1399–1407. doi: 10.1016/0040-4020(79)85034-6

[63] Paterson DA, Abberley JP, Harrison WT, et al. Cyanobiphenyl-based liquid crystal dimers and the twist-bend nematic phase. Liq Cryst. 2017;44:127–146. doi: 10.1080/02678292.2016.1274293

[64] Date RW, Imrie CT, Luckhurst GR, et al. Smectogenic dimeric liquid-crystals - the preparation and properties of the α,ω-bis(4-normal-alkylanilinebenzylidine-4'-oxy)alkane. Liq Cryst. 1992;12:203–238. doi: 10.1080/02678299208030393

[65] Emsley JW, Luckhurst GR, Shilstone GN. The orientational order of nematogenic molecules with a flexible core - a dramatic odd even effect. Molec Phys. 1984;53(4):1023–1028. doi: 10.1080/00268978400102811

[66] Imrie CT. Laterally substituted dimeric liquid-crystals. Liq Cryst. 1989;6:391–396. doi: 10.1080/02678298908034184

[67] Donaldson T, Staesche H, Lu ZB, et al. Symmetric and non-symmetric chiral liquid crystal dimers. Liq Cryst. 2010;37(8):1097–1110. doi: 10.1080/02678292.2010.494412

[68] Paterson DA, Xiang J, Singh G, et al. Reversible isothermal twist-bend nematic-nematic phase transition driven by the photoisomerization of an azobenzene-based non-symmetric liquid crystal dinner. J Am Chem Soc. 2016;138:5283–5289. doi: 10.1021/jacs.5b13331

[69] Pociecha D, Crawford CA, Paterson DA, et al. Critical behavior of the optical birefringence at the nematic to twist-bend nematic phase transition. Phys Rev E. 2018;98(5):052706. doi: 10.1103/PhysRevE.98.052706

[70] Riande E, Guzman J. Statistical properties of alternating copolymers .1. Dipole-moments of poly(thiodiethylene glycol) chains. Macromolec. 1979;12:952–956. doi: 10.1021/ma60071a033

[71] Emsley JW, De Luca G, Lesage A, et al. The structure and conformation of a mesogenic compound between almost zero and almost complete orientational order. Liq Cryst. 2007;34(9):1071–1093. doi: 10.1080/02678290701565834

[72] Bondi A. Van der Waals volumes and radii. J Phys Chem. 1964;68(3):441–451. doi: 10.1021/j100785a001

[73] Martinez-Gomez A, Perez E, Bello A. Synthesis of copolybibenzoates with thioether and ether groups in the flexible spacers. Polym Int. 2005;54(8):1196–1204. doi: 10.1002/pi.1831